Journal of Advanced Research 56 (2024) 57–68

Contents lists available at ScienceDirect

Journal of Advanced Research

journal homepage: www.elsevier.com/locate/jare

Original Article

Targeted m^{6}A demethylation of *ITGA6* mRNA by a multisite dCasRx–m^{6}A editor inhibits bladder cancer development

Xiaoling Ying [a,b,1], Yapeng Huang [a,1], Bixia Liu [a], WenYu Hu [a], Ding Ji [c], Cong Chen [a], Haiqing Zhang [a], Yaomin liang [a], Yifan lv [d], Weidong Ji [a,*]

[a] Center for Translational Medicine, The First Affiliated Hospital, Sun Yat-sen University, Guangzhou 510080, China
[b] Department of Urology, The First Affiliated Hospital, Sun Yat-sen University, Guangzhou 510080, China
[c] Department of Otolaryngology, The First Affiliated Hospital, Sun Yat-sen University, Guangzhou 510080, China
[d] Department of Urology, Minimally Invasive Surgery Center, The First Affiliated Hospital of Guangzhou Medical University, Guangdong Key Laboratory of Urology, Guangzhou 510230, China

HIGHLIGHTS

- We for the first time designed a targeted ITGA6 multi-locus guide (g) RNA and established a bidirectional deactivated RfxCas13d (dCasRx)-based m^{6}A-editing platform.
- The dCasRx–m^{6}A editors have a high on-target efficiency.
- Multi-target demethylation using dCasRx–m^{6}A editors reduces ITGA6 translation.
- Multi-target demethylation of ITGA6 mRNA inhibits BCa progression.
- Adeno-associated delivery of dCasRx–ALKBH5-CD and ITGA6-multi-gRNA inhibits BCa progression.

GRAPHICAL ABSTRACT

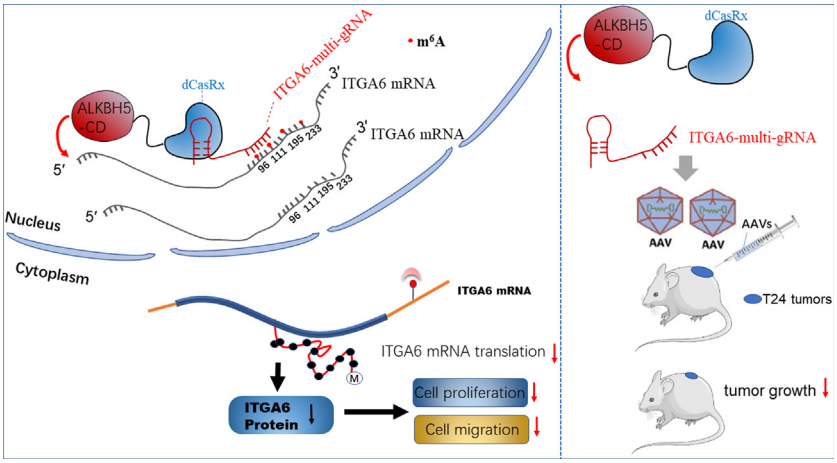

ARTICLE INFO

Article history:
Received 26 September 2022
Revised 22 February 2023
Accepted 22 March 2023
Available online 30 March 2023

Keywords:
dCasRx
N^6-methyladenosine
Multisite

ABSTRACT

Introduction: N6-methyladenosine (m^{6}A) modification contributes to the pathogenesis and development of various cancers, including bladder cancer (BCa). In particular, integrin ∝6 (ITGA6) promotes BCa progression by cooperatively regulating multisite m^{6}A modification. However, the therapeutic effect of targeting *ITGA6* multisite m^{6}A modifications in BCa remains unknown.
Objectives: We aim to develop a multisite dCasRx– m^{6}A editor for assessing the effects of the multisite dCasRx–m^{6}A editor targeted m^{6}A demethylation of ITGA6 mRNA in BC growth and progression.
Methods: The multisite dCasRx– m^{6}A editor was generated by cloning. m^{6}A-methylated RNA immunoprecipitation (meRIP), luciferase reporter, a single-base T3 ligase-based qPCR-amplification, Polysome profiling and meRIP-seq experiments were performed to determine the targeting specificity of the

Peer review under responsibility of Cairo University.

* Corresponding author.
E-mail address: jiweidong@mail.sysu.edu.cn (W. Ji).

[1] First two authors have contributed equally to the manuscript.

https://doi.org/10.1016/j.jare.2023.03.010

ITGA6
Bladder cancer
Adeno-associated viral

multisite dCasRx–m^{6}A editor. We performed cell phenotype analysis and used *in vivo* mouse xenograft models to assess the effects of the multisite dCasRx–m^{6}A editor in BC growth and progression.

Results: We designed a targeted *ITGA6* multi-locus guide (g)RNA and established a bidirectional deactivated RfxCas13d (dCasRx)-based m^{6}A-editing platform, comprising a nucleus-localized dCasRx fused with the catalytic domains of methyltransferase-like 3 (METTL3-CD) or α-ketoglutarate-dependent dioxygenase alkB homolog 5 (ALKBH5-CD), to simultaneously manipulate the methylation of *ITGA6* mRNA at four m^{6}A sites. The results confirmed the dCasRx–m^{6}A editor modified m^{6}A at multiple sites in *ITGA6* mRNA, with low off-target effects. Moreover, targeted m^{6}A demethylation of ITGA6 mRNA by the multisite dCasRx–m^{6}A editor significantly reduced BCa cell proliferation and migration *in vitro* and *in vivo*. Furthermore, the dCasRx–ALKBH5-CD and *ITGA6* multi-site gRNA delivered to 5-week-old BALB/cJNju-Foxn1nu/Nju nude mice via adeno-associated viral vectors significantly inhibited BCa cell growth.

Conclusion: Our study proposes a novel therapeutic tool for the treatment of BC by applying the multisite dCasRx–m^{6}A editor while highlighting its potential efficacy for treating other diseases associated with abnormal m^{6}A modifications.

Introduction

Bladder cancer (BCa) is among the most prevalent types of urinary tract malignancies, with an estimated 549,393 newly diagnosed cases and 199,922 deaths in 2018 worldwide [1]. Although 75 % of the patients have non-muscle-invasive BCa (NMIBC), ∼25 % present with MIBC [2]. Most patients with non-MIBC achieve remission following transurethral resection of the bladder tumor, the 5-year recurrence rate ranges from 60 % to 90 % [3,4]. Even in patients with MIBC who undergo aggressive radical cystectomy, the 5-year mortality rate remains at 50 % to 70 % [5]. Given that the high recurrence and drug resistance rates are the primary characteristicsof BCa [6], an urgent need exists for the development of novel BCa therapy strategies.

N6-methyladenosine (m^{6}A) is the most abundant RNA post-transcriptional modification in eukaryotes [7]. This modification is catalyzed by a methyltransferase complex that includes methyltransferase-like 3 (METTL3) and METTL14, and it is removed by demethylases, such as fat mass and obesity-associated protein and α-ketoglutarate-dependent dioxygenase alkB homolog 5 (ALKBH5) [8]. Different reader proteins specifically recognize m^{6}A modifications and mediate various biological functions, such as regulating mRNA stability, translation, pre-mRNA splicing, 3′ processing, and long noncoding RNA processing [9–12]. Additionally, the m^{6}A modification plays a critical role in various physiological and pathological processes, including tumorigenesis [8,13], with recent evidence indicating that abnormal m^{6}A modifications are closely related to human cancers [14–16]. METTL3 is highly expressed in BCa and promotes its progression by regulating target gene expression, including that of *AF4/FMR2 family member 4*, *CUB-domain-containing protein 1* (*CDCP1*), and *integrin α6* (*ITGA6*) [17–19]. ALKBH5 inhibits BCa by regulating the casein kinase 2α-mediated glycolysis in an m^{6}A-dependent manner [20]. However, although m^{6}A has been shown to participate in BCa formation and development, the therapeutic effect of targeting m^{6}A in BCa remains unknown.

ITGA6 is a 150- kDa transmembrane protein, a member of the integrin family, and is highly expressed in metastatic breast cancer, wherein it promotes invasion and tumor-initiating cell activities [21]. Additionally, an elevated ITGA6β4 expression increases cell invasion and reduces survival in patients with non-small cell lung cancer [22]. Moreover, ITGA6 is closely associated with human cervical cancer progression [23]. Meanwhile, we previously reported that the m^{6}A modification promotes ITGA6 translation, upregulates ITGA6 protein expression, and enhances BCa progression [18]. We also identified multiple m^{6}A sites in the 3′ untranslated region (UTR) of *ITGA6* mRNA and reported that single mutations in one m^{6}A loci do not alter ITGA6-translation efficiency, whereas simultaneous mutations at multiple sites reduce its translation [18]. These results suggest that multi-locus m^{6}A modifications cooperatively regulate ITGA6 expression and promote the development of BCa. Therefore, targeted *ITGA6* multisite m^{6}A modifications might represent a novel strategy for BCa therapy. However, the methods of targeting multisite m^{6}A modifications efficiently and simultaneously remain unexplored.

The CRISPR-associated nuclease Cas13 family is a robust platform for the binding and cleavage of RNA by guide (g)RNA [24]. Cas13 proteins have four isoforms—Cas13a(C2c2), Cas13b, Cas13c, and Cas13d, all of which have smaller molecular weights than the molecular weight of cas9. Cas13d is a relatively small class II CRISPR effector found in mammalian cells (average length: 930 amino acids [20 % smaller than Cas13a–c and 33 % smaller than Cas9]) [25]. Additionally, Cas13d RNA cleavage does not depend on the protospacer-flanking sequence (similar to the protospacer-adjacent motif [PAM] sequence of Cas9), which greatly increases its application. RfxCas13d (CasRx), which belongs to the Cas13d family, is the smallest Cas enzyme and exhibits a high knockdown efficiency and low off-target effects [25]. Moreover, CasRx can be easily packaged into adeno-associated virus (AAV) vectors owing to its small size. Indeed, Zhou et al. [26] confirmed the ability of CasRx to be packaged into an AAV vector and introduced into adult animals to silence RNA activity, which subsequently resulted in the regeneration of optic ganglion cells and vision restoration in mouse models of permanent visual impairment. AAV vectors demonstrate high degrees of safety and low immunogenicity and are applicable in a wide host-cell range. They are also, easy to produce and show high penetration, long-term expression, and site-specific integration, which makes them one of the most promising delivery tools for gene therapy.

In this study, we fused the catalytic domains of METTL3 or ALKBH5 (METTL3-CD and ALKBH5-CD, respectively) with deactivated (d)CasRx and designed *ITGA6* gRNA to achieve the specific manipulation of multiple loci in *ITAG6* for m^{6}A modification with low off-target efficiency. More specifically, dCasRx–METTL3-CD and dCasRx–ALKBH5-CD were packaged into lentivirus vectors and applied to *in vitro* and *in vivo* assays to demonstrate the demethylation activity and the efficacy of dCasRx–ALKBH5-CD along with the multi-locus *ITGA6* gRNA in downregulating BCa cell proliferation and migration. Moreover, *in vivo*, the dCasRx–ALKBH5-CD and ITGA6 multi-site gRNA delivered to T24 tumor-bearing mice via AAV vectors significantly inhibited tumor growth. Collectively, this study highlights the utility of the multisite dCasRx– m^{6}A editor as a novel strategy for BCa treatment.

Materials and methods

Plasmid constructs

Wild-type (WT) and mutated CDs (D395A for mutated METTL3; H204A for mutated ALKBH5) in METTL3-CD and ALKBH5-CD were synthesized with a short linker sequence and cloned into a *NheI*-digested lentiviral expression vector EF1a-dCasRx-2A-enhanced green fluorescent protein (EGFP) (#109050; Addgene, Watertown, MA, USA). Fusion genes of the gRNA scaffold for CasRx, harboring *BsmBI* sites for guide cloning and the central polypurine tract (cPPT), as well as the central termination sequence (CTS) of human immunodeficiency virus (HIV) were synthesized and inserted into the *BsmBI* and *PspxI*-digested lentiviral expression plasmid lentiGuide-Hygro-mTagBFP2 (Addgene_99374).

The dCasRx-ALKBH5-CD-2A-EGFP fusion genes were amplified from the constructed vector and ligated into the *BamHI* and *KpnI*-digested AAV vector pHBAAV-CMV-MCS-3flag (termed $AAV^{dCasRx\text{-}ALKBH5\text{-}CD}$). The gRNAs targeting four m^6A sits in the 3′ UTR of *ITGA6* (96, 111, 195, and 233 bp from the 5′ end of the *ITGA6* 3′ UTR) were designed according to previously described methods [27]. The ITGA6-multi-gRNA for CasRx, containing four independent Pol-III promoters (human U6 promoter, H1, mouse U6 promoter and 7SK), was synthesized (the sequence shown in Supplementary material) and incorporated into the *BsmB*I-digested pLV GG hUbC-dsRED (#84034; Addgene) lentiviral expression vector (termed Lenti-ITGA6-multi-gRNA) and inserted into an *EcoR*I- and a *Hind*III-digested AAV vector pHBAAV-CMV-MCS-T2A-ZsGreen (termed $AAV^{ITGA6\text{-}multi\text{-}gRNA}$). The primer sequences used for PCR amplification are summarized in Supplementary Table S1, and the sequences used for the gRNAs are shown in Supplementary Table S2.

Establishment of stable cell lines

Human uroepithelial (SV-HUC-1) and 293 T (ECACC Cat# 12022001, RRID: CVCL_0063) cells were purchased from the American Type Culture Collection (Manassas, VA, USA). The BCa cell line T24 was acquired from the Institute of Cell Biology, Chinese Academy of Sciences (Shanghai, China). Stable cell lines were created according to our previously described methods [18]. Lentiviral vectors expressing dCasRx–METTL3-CD-EGFP, dCasRx–ALKBH5-CD-EGFP, or gRNAs targeting *ITGA6* were generated, as described. For virus transduction, the target plasmid and packaging vectors were co-transfected into 293 T cells. The target cells were transduced to construct stable cell lines using8 μg/mL polybrene (Sigma-Aldrich, Hamburg, Germany). After 72 h, the cells were selected with puromycin (2 μg/mL) or hygromycin for 5 to 7 days.

m^6A-methylated RNA immunoprecipitation (meRIP)

Cells stably expressing the dCasRx m^6A editors were cultured, as described, and passaged at an 80 % confluency. Total RNA was extracted from the cells using TRIzol reagent (Invitrogen), and the mRNA was isolated using the GenElute mRNA miniprep kit (Sigma-Aldrich). The mRNA (10 μg) was then fragmented into 200- to 300-nt fragments using an RNA fragmentation kit (Ambion, Austin, TX, USA) and immunoprecipitated with Protein Magnetic A/G beads (Thermo Fisher Scientific) coated with an anti-m^6A antibody (Synaptic Systems Cat# 202 003, RRID: AB_2279214). After immunoprecipitation, RNA was washed and eluted from the beads using an m^6A elution buffer (Sigma-Aldrich); the purified RNA fragments were then used for RT-qPCR analysis.

MeRIP-seq and analysis

As previously described [28], m^6A-modified RNA was extracted from total RNA using the meRIP method. The SMARTer Stranded Total RNA-Seq Kit (Takara, #634413) was used to generate the library, while NovaSeq 6000 (Illumina) was employed for paired-end 150 cycle sequencing. MeRIP-seq raw data were trimmed with TrimGalore software v.0.6.6, and trimmed reads were then aligned with the human genome GRCh38 using the STAR aligner. Differentially methylated regions were obtained using the R package.

Single-base validation using a ligase-based method

T24 cells stably expressing dCasRx–ALKBH5-CD and gRNAs were generated using the constructed lentivirus. According to the previously described methods for single-base T3 ligation [29–31], the DNA probes L (left) and R (right) were designed (Supplementary Table S3). The ligation reaction was performed in an 8 μL volume containing 300 ng total RNA, 20 nM probe L, 20 nM probe R, and 1× T3 ligation buffer (New England Biolabs). The reaction mixture was heated at 85 °C for 3 min and then incubated at 35 °C for 10 min. Subsequently, T3 DNA ligase (50 U) and 1× ligation buffer were added to bring the final volume to 10 μL; then the mixture was incubated at 35 °C for 10 min and placed on ice. For PCR amplification, 1 μL ligated product was amplified with 2× Taq mix (Vazyme Biotech, Nanjing, China) and the following steps: initial denaturation at 94 °C for 2 min, followed by 35 cycles of 94 °C for 45 s, 58 °C for 45 s, and 72 °C for 45 s. All PCR products were visualized by performing gel electrophoresis using 2 % agarose gel and 1× Tris-acetate-EDTA buffer.

Dual-luciferase reporter assay

The 3′ UTR of the *ITGA6* gene was cloned from human umbilical vein endothelial cells into the psiCHECK-2 vector (Addgene_35672) to create psiCHECK-2-ITGA6-3′-UTR. 293 T and SV-HUC-1 cells were cultured, as described [18], and passaged at 80 % confluency. A total of 300,000 cells were plated in each well of a 24-well tissue culture plate. After 24 h, the cells were co-transfected with dCasRx-METTL3-CD, dCasRx-dMETTL3-CD, gRNAs, or psiCHECK-2-ITGA6-3′-UTR plasmids at a mass ratio of 5:3:1 using Lipofectamine 3000 (Life Technologies). After 48 h, the cells were washed with PBS and lysed with a reporter lysis buffer (Promega). Relative luciferase activity of the lysates was measured using the Dual-Glo luciferase assay system (Promega) on a SYNERGY microplate reader (BioTek, Winooski, VT, USA).

Western blotting and immunostaining

Western blot and immunostaining assays were conducted as previously described [32]. The antibodies using for western blotting were as follows: anti-rabbit METTL3 (Proteintech, Cat# 15073–1-AP), anti-rabbit ITGA6 (1:1000; 3750S; Cell Signaling Technology, Danvers, USA), anti-rabbit ALKBH5 (1:1000; 80283S; Cell Signaling Technology), and anti-rabbit β-actin (1:1000; 4970 T; Cell Signaling Technology). For immunostaining assays, Cells were fixed with 4 % paraformaldehyde, blocked with 1 % BSA, and incubated overnight at 4 °C with anti-rabbit ITGA6 antibody (1:200; 3750S; Cell Signaling Technology), followed by incubation with Alexa Fluor 568 donkey anti-rabbit IgG (H + L) (1:1000; 1891789; Invitrogen). Nuclear staining was performed using 1 × 4′,6-diamidino-2-phenylindole (S2110; Solarbio, Beijing, China), and images were obtained with a confocal microscope (LSM880; Carl Zeiss, Oberkochen, Germany).

Polysome profiling and RT-qPCR

Polysome profiling was performed as described previously [32]. Fractions were collected and purified with TRIzol reagent (Life Technologies), and reverse-transcribed to cDNA using TransScript All-in-One first-strand cDNA synthesis SuperMix for qPCR (Vazyme Biotech, Nanjing, China). RT-qPCR was carried out with Fast SYBR Green PCR master mix (Vazyme Biotech, Nanjing, China). The primers used for RT-qPCR are listed in Supplementary Table S4.

Proliferation assay

Stable cells (3000/well) expressing dCasRx–ALKBH5-CD and ITGA6 multi-locus guide (g)RNA were seeded in 96-well plates and incubated for 0–5 days. Cell proliferation was determined using the MTS assay (Promega). Briefly, 20 μL of MTS was added to each well after 24, 48, 72, and 96 h, after which, the plate was incubated for an additional 2 h. Absorbance at 490 nm was determined using a Synergy microplate reader (BioTek).

Migration assay

Scratch assays were performed on a real-time cell imaging system (Essen Bioscience, Ann Arbor, MI, USA). The cells (1×10^5/well) were grown to confluence in 96-well Essen ImageLock plates (Essen Bioscience) in a standard CO_2 incubator. A 96-pin Wound Maker was used to make precise and reproducible wounds in the cell monolayer, after which the plates were washed with cold PBS and scanned every hour for 24 h. Images were acquired using phase-contrast imaging. Data were evaluated by determining the relative wound density and analyzed using the GraphPad Prism software.

Sphere formation assay

The sphere formation assay was performed as described previously [18]. Briefly, Cells were plated in 96-well ultralow attachment culture dishes (315, 625, 1250, 2500 or 5000 cells/well) in cancer sphere medium and cultured for 8 days. The sizes of tumorspheres were observed and recorded each day.

Animal experiments

To induce tumor formation, 5×10^6 cells were subcutaneously implanted into 5-week-old BALB/cJNju-Foxn1nu/Nju nude mice (Nanjing Biomedical Research Institute, Nanjing University). Tumor growth was assessed each week. The mice were sacrificed 4 weeks after surgery. Tumor volume was calculated as follows: tumor volume = length × width^2 × 0.52. For generating the cancer metastasis model, we injected 1×10^6 cells into 5-week-old nude mice by tail vein injection and observed lung metastases after six weeks. The AAV$^{dCasRx\text{-}ALKBH5\text{-}CD}$ and AAV$^{ITGA6\text{-}multi\text{-}gRNA}$ vectors were packaged into AAV serotype 8 viruses by Han Heng Biotechnology (Shanghai). Next, 5×10^5 T24 cells were subcutaneously injected into 5-week-old BALB/cJNju-Foxn1nu/Nju nude mice. After 1 week, the mice were randomly divided into two groups—AAV-Ctrl and AAV-dCasRx-ALKBH5. In the control group, mice were intratumorally injected with 1×10^{11} vp AAV^{GFP} every second day a total of three times. In the experimental group, mice were injected with AAV$^{dCas\ \ Rx\text{-}ALKBH5\text{-}CD}$ and AAV$^{ITGA6\text{-}multi\text{-}gRNA}$ using the same approach. Tumor weight and size were measured after 30 days. The livers and kidneys were collected for pathological analysis.

Ethics statement

All animal experiments were performed according to all Institutional and National Guidelines for care and use of animals, which were also approved by the Institutional Ethics Committee for Clinical Research and Animal Trials of the First Affiliated Hospital of Sun Yat-sen University ([2017]257).

Statistical analysis

Statistical analyses were performed using the GraphPad Prism software (GraphPad Prism,). All experiments were independently repeated at least thrice. The data were presented as mean ± standard error of the mean and analyzed via an unpaired Student's *t*-test or repeated-measures ANOVA. *P*-values < 0.05 were considered statistically significant.

Results

Design of the dCasRx–m^{6}A editors and a single lentiviral/AAV vector for multiplex genome engineering

Given that METTL3 contains one catalytic subunit within the METTL3:METTL14 m^{6}A methyltransferase complex, we hypothesized that METTL3 alone could serve as a binding-impaired methyltransferase that would represent an ideal target for fusion with an RNA-binding protein, such as dCasRx. To test this hypothesis, we designed dCasRx–m^{6}A editors for RNA targeting, with METTL3-CD or ALKBH5-CD fused to the EGFP-tagged RNA-binding protein dCasRx (Fig. 1A); mutated versions of the respective CDs were employed as negative controls. The fusion genes of the gRNA scaffold for CasRx harboring *BsmB*I sites for guide cloning and the CPPT/CTS of HIV were inserted into the lentiviral expression vector lentiGuide-Hygro-mTagBFP2 to construct a single-site-targeting RNA plasmid (Fig. 1A).

Although most genes harbor multiple m^{6}A-modification sites, it remains challenging to deliver multiple gRNAs efficiently and simultaneously for m^{6}A modification. Thus, to evaluate the function of the multisite m^{6}A editor, we developed a single lentiviral or AAV vector that efficiently expressed up to four gRNAs (Fig. 1B). Four previously validated m^{6}A-modification sites (#96, #111, #195, and #233) in *ITGA6* mRNA were selected [18] to construct the Lenti-ITGA6-multi-gRNA and AAV-ITGA6-multi-gRNA vectors, which expressed four gRNAs under the control of human U6, H1, mouse U6, and 7SK promoters (Fig. 1B). Four independent Pol-III promoters achieved maximum expression efficiency of each gRNA [33]. We hypothesized that nucleus-localized dCasRx fusions with truncated m^{6}A editors will directly introduce or remove m^{6}A modifications at the sites specified by a CasRx–gRNA (Fig. 1C).

Validation of the dCasRx–m^{6}A editors

Our previous work showed that METTL3 is expressed at low levels in SV-HUC-1 cells and ALKBH5 is low expressed in T24 cells [18]. To evaluate these candidate dCasRx–m^{6}A constructs in human cells, we first transfected the lentiviral vector expressing the dCasRx–METTL3-CD-EGFP fusion protein into SV-HUC-1 cells and the dCasRx–ALKBH5CD-EGFP lentiviral vector into T24 cells. Determination of the fluorescence intensity of each fusion protein revealed that the dCasRx–METTL3CD-EGFP and dCasRx–ALKBH5CD-EGFP fusion proteins primarily localized to the nucleus, based on their respective nuclear-localization signal (Fig. 2A). We further validated the expression of the dCasRx–m^{6}A editors dCasRx–METTL3CD-EGFP and dCasRx–ALKBH5CD-EGFP via western blotting. Results confirmed successful expression of the fusion

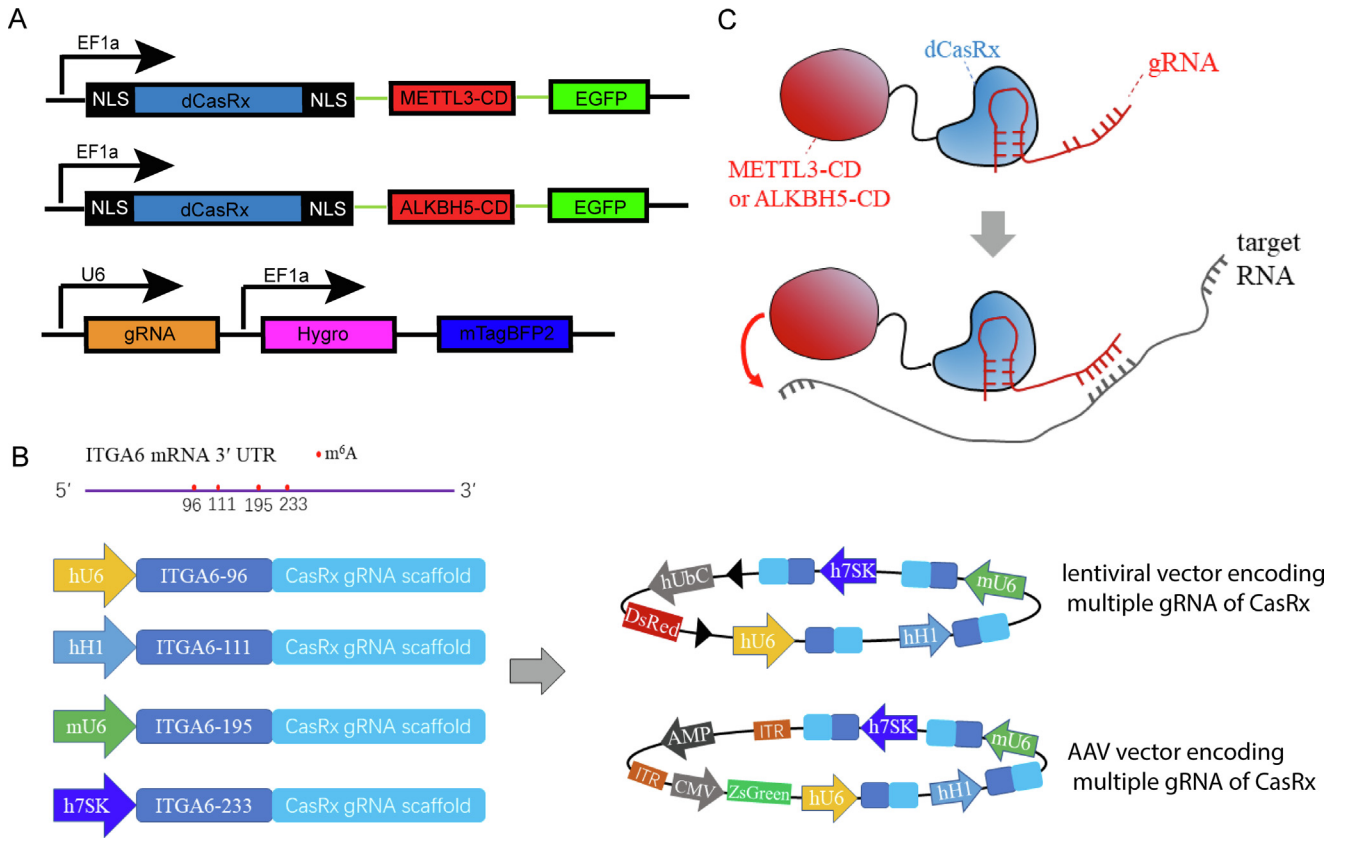

Fig. 1. Modular design of the dCasRx m^{6}A editors mediating mRNA targeting. (A) Upper panel: schematic representation of the METTL3 catalytic domain (METTL3-CD), deactivated CasRx (dCasRx) and EGFP fusion proteins. Middle panel: schematic representation of the ALKBH5 catalytic domain (ALKBH5-CD), deactivated CasRx (dCasRx) and EGFP fusion proteins. Lower panel: single-site gRNA construct with hygromycin and tagBFP2. (B) Golden Gate assembly of lentiviral/AAV vector encoding multiple gRNA of ITGA6 expression cassettes. (C) Schematic representation of the RNA-targeting dCasRx m^{6}A editors, including nuclease-inactive CasRx (dCasRx), METTL3 catalytic domain (METTL3-CD), or ALKHB5 catalytic domain (ALKBH5-CD), as well as fluorescent protein EGFP fusion proteins, and a gRNA.

proteins in SV-HUC-1 and T24 cells (Fig. 2B and C). We constructed fusion proteins comprising dCasRx and a catalytically dead mutant of METTL3-CD D395A (dMETTL3-CD) or demethylase-dead ALKBH5-CD H204A (dALKBH5-CD) as controls. To assess whether the dCasRx–METTL3-CD-EGFP or dCasRx–ALKBH5CD-EGFP affects m^{6}A modification at the global level, dot blot assays were conducted in SV-HUC-1 and T24 cells. The results indicated that the overall level of m^{6}A were unaffected by dCasRx–METTL3-CD-EGFP or dCasRx–ALKBH5CD-EGFP (Supplementary Fig. S1). To test the expression of each gRNA from the single lentiviral vector(Lenti-ITGA6-multi-gRNA) expressing four independent ITGA6-targeting gRNAs from the four independent Pol III promoters, we first transfected the lentiviral vector (Lenti-ITGA6-multi-gRNA) into 293 T cells and then observed expression of each gRNA using RT-PCR. The result showed that each gRNA was highly expressed at similar level in 293 T cells transfected with Lenti-ITGA6-multi gRNA (Supplementary Fig. S2). Furthermore, we validate the expression of each gRNA in T24 cells stably expressing ITGA6-multi-gRNA and observed expression of each gRNA which had a similar expression level (Fig. 2 D).

We previously reported that four m^{6}A-modification sites (#96, #111, #195, and #233) are present in the 3′ UTR and promote the translation of *ITGA6* mRNA(18). To determine whether dCasRx–METTL3-CD facilitates the translation of targeted mRNA, we performed dual-luciferase reporter assays. Specifically, we designed several gRNAs targeting 30-bp sites that end 1–22 bp away from 5′ of the target adenine (ITGA6-96) to investigate the editing window of the dCasRx–METTL3CD-EGFP construct (Supplementary Fig. S3A). Following transfection of dCasRx–METTL3CD-EGFP, ITGA6-gRNAs and the luciferase vector containing the WT or mutant *ITGA6* 3′ UTR into HEK293T cells, we found that luciferase activity was higher in the target groups than in the mutant groups (Supplementary Fig. S3B). Moreover, cells with ITGA6-gRNA that ended 10 bp away from 5′ of the target adenine showed the highest luciferase activity (Supplementary Fig. S3B). Based on these results, we designed gRNAs that ended 10 bp away from 5′ of the target adenine.

We previously reported that simultaneous mutations at four m^{6}A-modification sites in *ITGA6* mRNA significantly reduce luciferase activity relative to that of the WT control, whereas mutation at any one site alone does not affect luciferase activity(18). Therefore, we selected ITGA6-gRNA or ITGA6-multi-gRNA to confirm whether targeting of multiple loci simultaneously results in greater luciferase activity than that achieved by targeting a single site. The dual-luciferase reporter assay indicated that in ITGA6-gRNA groups METTL3-CD construct, but not the dMETTL3-CD construct, had enhanced luciferase activity relative to the non-target group (λ2-gRNA; Fig. 2E). Interestingly, the highest luciferase activity was observed in the group that targeted multiple sites (Fig. 2E). These results suggest that multi-locus m^{6}A modifications cooperatively regulate *ITGA6* expression.

We then tested the effect of dCasRx epitranscriptomic multi-locus editors by introducing or removing m^{6}A modifications in human cells. We first generated stable SV-HUC-1 cell lines overexpressing dCasRx–METTL3-CD and a negative control gRNA (“λ2” gRNA) or ITGA6-multi-gRNA using lentiviral vectors, followed by meRIP– quantitative reverse transcription (RT-qPCR) analysis to quantify the enrichment of the *ITGA6* RNA fragments. The results

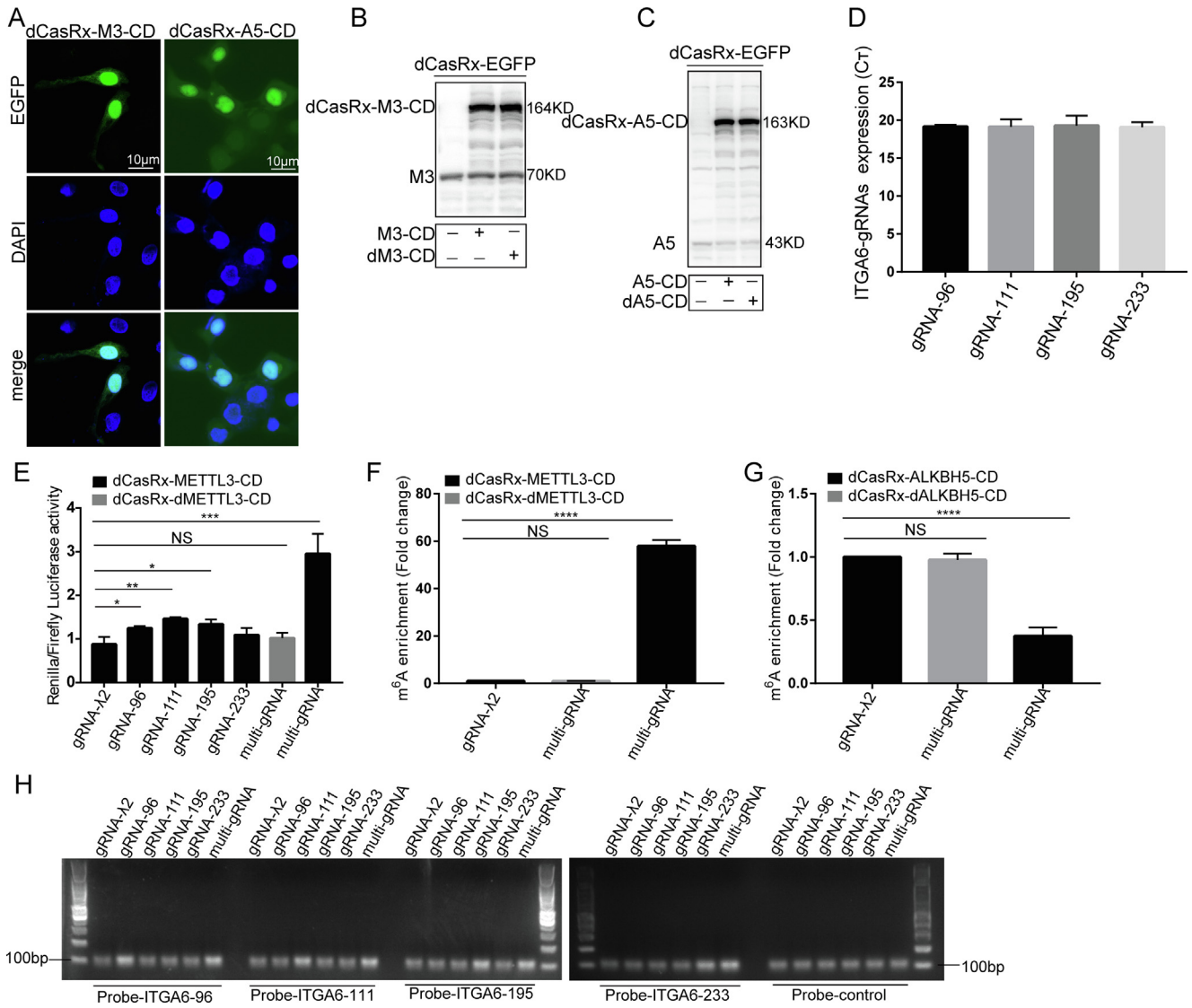

Fig. 2. Validation of dCasRx-m^{6}A editors. (A) Representative immunofluorescence images of SV-HUC-1 cells transfected with EGFP-tagged dCasRx-METTL3-CD and T24 cells transfected with EGFP-tagged dCasRx -ALKBH5-CD. Scale bars, 10 μm. (B) Western blot results of dCasRx-METTL3-CD and dCasRx-dMETTL3-CD in living SV-HUC-1 cells. (C) Western blot results of dCasRx-ALKBH5-CD and dCasRx-dALKBH5-CD in living T24 cells. (D) RT-qPCR revealed that each gRNA was highly expressed at similar level in T24 cells stably expressing ITGA6-multi-gRNA. (E) Dual luciferase reporter assay in SV-HUC-1 cells treated with the luciferase vector containing the WT ITGA6 3′ UTR, dCasRx-METTL3-CD, dCasRx-dMETTL3-CD, and gRNAs. The dual-luciferase reporter assay showed that dCasRx-METTL3-CD had enhanced luciferase activity in ITGA6-gRNA groups relative to the non-target group (λ2-gRNA). ITGA6-multi-gRNA resulted in the highest luciferase activity. (F) me-RIP assay showed that m^{6}A abundance of ITGA6 was increased in SV-HUC-1 cells stably transfected with dCasRx-METTL3-CD and ITGA6-multi-gRNA compared with λ2-gRNA group. (G) me-RIP assay showed that m^{6}A abundance of ITGA6 was reduced in T24 cells stably transfected with dCasRx-ALKBH5-CD and ITGA6-multi-gRNA compared with λ2-gRNA group. (H). Validation results of four ITGA6 m^{6}A sites via single-based T3 ligase-based qPCR amplification in T24 cells stably expressing dCasRx-ALKBH5-CD and ITGA6-gRNAs. The results indicated that the dCasRx-ALKBH5-CD with the target gRNAs reduced methylation at the corresponding m^{6}A-modification sites. M3(METTL3), A5(ALKBH5). *P < 0.05, **P < 0.01, ***P < 0.001, ****P < 0.0001.

demonstrated greater enrichment of *ITGA6* RNA in cells expressing dCasRx–METTL3CD and ITGA6-multi-gRNA than in control cells expressing dCasRx–METTL3-CD and "λ2" guide (g)RNA (Fig. 2F). Similarly, transduction of T24 cells with dCasRx–ALKBH5-CD, ITGA6-multi-gRNA, or control lentiviral vectors revealed that co-transduction with dCasRx–ALKBH5CD and ITGA6-multi-gRNA reduced *ITGA6* m^{6}A methylation relative to that observed in the non-target control ("λ2" gRNA) (Fig. 2G). By contrast, transduction with catalytically dead constructs (dCasRx-dMETTL3-CD and dCasRx-dALKBH5-CD) did not alter the methylation level of *ITGA6* (Fig. 2F and G). These results suggested that the dCasRx–m^{6}A editors could successfully insert or remove m^{6}A modifications.

To assess site-specific m^{6}A modifications, we used a single-base T3 ligase-based quantitative polymerase chain reaction (qPCR)-amplification method (Supplementary Fig. S4A), with probes L and R designed against the *ITGA6* 3′ UTR at four m^{6}A-modification sites (#96, #111, #195, and #233). Simultaneously, we designed probes against an unmethylated adenine site as controls. Cells harboring dCasRx–ALKBH5-CD and the target corresponding m^{6}A sites gRNAs had larger amounts of PCR products than the control cells (Fig. 2H and Supplementary Fig. S4B–E), indicating that the dCasRx-ALKBH5-CD with the target gRNAs reduced methylation at the corresponding m^{6}A-modification sites. In control experiments, transduction with dCasRx–ALKBH5-CD and target gRNAs did not alter the m^{6}A levels at unmethylated adenine sites (Fig. 2H and Supplementary Fig. S4F), confirming that a low-risk, off-target, and site-specific m^{6}A modification was edited by dCasRx–ALKBH5-CD with the help of the target gRNAs. These

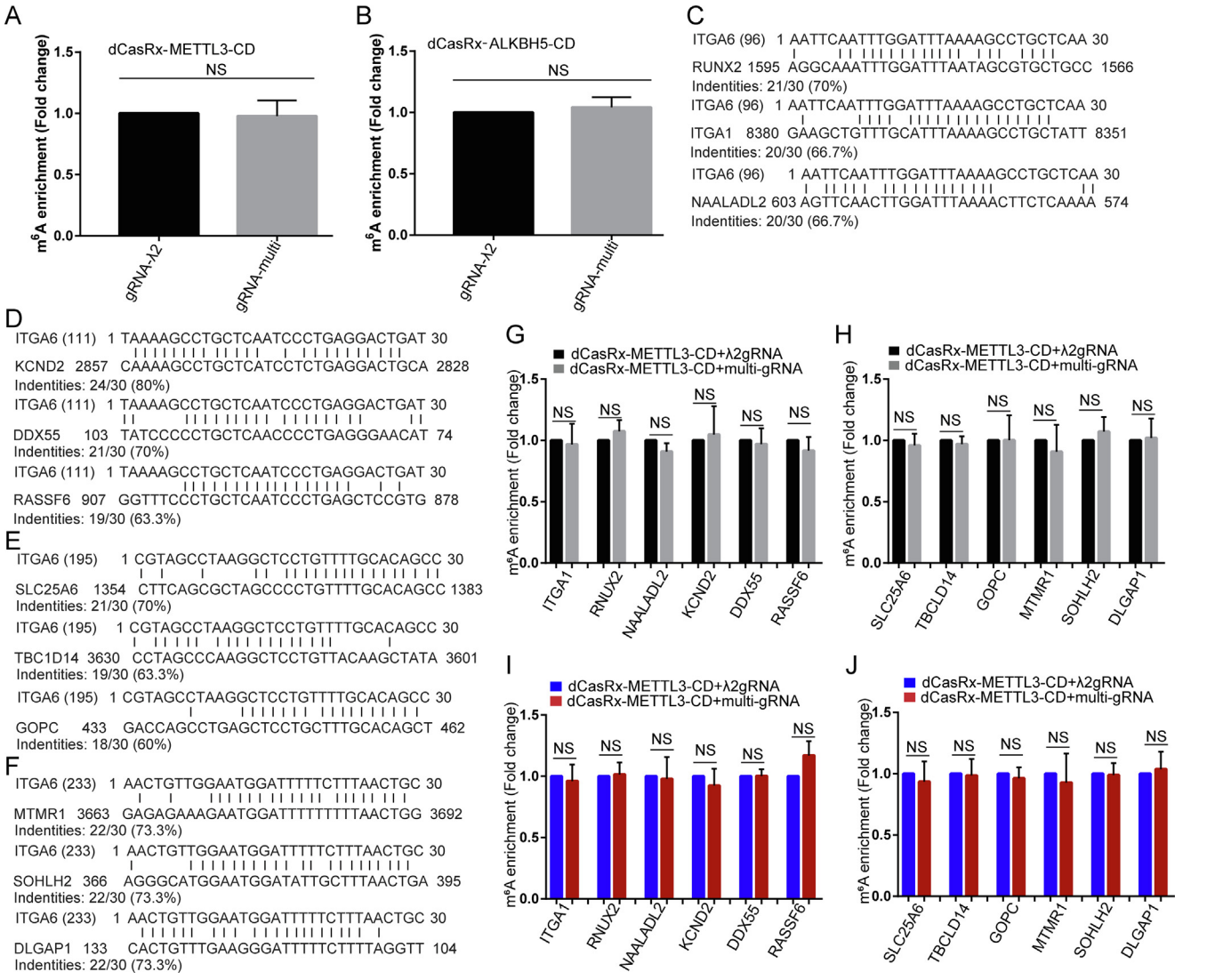

Fig. 3. Assessment of dCasRx-m^{6}A editor off-target effects. (A) m^{6}A abundance of ITGA6 unmethylated A site in SV-HUC-1 cells stably expressing dCasRx-METTL3-CD and ITGA6-multi-gRNA. (B) m^{6}A abundance of ITGA6 unmethylated A site in T24 cells stably expressing dCasRx-ALKBH5-CD and ITGA6-multi-gRNA. (C) Sequence alignment between ITGA6-gRNA-96 targeting sequences and ITGA1, RNUX2, NALADL2. (D) Sequence alignment between ITGA6-gRNA-111 targeting sequences and KCND2, DDX55, RASSF6. (E) Sequence alignment between ITGA6-gRNA-195 targeting sequences and SLC25A6, TBCLD14, GOPC. (F) Sequence alignment between ITGA6-gRNA-233 targeting sequences and MTMR1, SOHLH2 or DLGAP1. (G, H) SV-HUC-1 cells were stably transfected with dCasRx-METTL3CD and λ2-gRNA or ITGA6-multi-gRNA. MeRIP assays showed that no significant difference was observed in m^{6}A levels between SV-HUC-1 cells transfected with ITGA6-multi-gRNA and cells transfected with λ2-gRNA at these off-target sites. (I, J) T24 cells were stably transfected with dCasRx-ALKBH5CD and λ2-gRNA or ITGA6-multi-gRNA. m^{6}A levels were detected using MeRIP-qRT-PCR. No significant difference was observed in m^{6}A levels at these off-target sites. All qRT-PCR data are presented as means ± SEM. n = 3.

data indicated that the dCasRx epitranscriptomic editors with target gRNAs could successfully manipulate m^{6}A levels at specific single or multiple sites.

Assessment of off-target effects of the dCasRx–m^{6}A editors

To evaluate the off-target effects of the dCasRx–m^{6}A editors, we designed primers against the unmethylated adenine site of *ITGA6* and performed meRIP–RT-qPCR assays. The results showed that transduction with dCasRx–METTL3-CD or dCasRx–ALKBH5-CD did not affect m^{6}A levels at the unmethylated adenine site (Fig. 3A and B), suggesting a low off-target effect of the dCasRx–m^{6}A editors. We then predicted the top three off-target sequences similar to each ITGA6-gRNA using BLASTN (https://blast.ncbi.nlm.nih.gov/) and detected these sites using meRIP–qPCR (Fig. 3C-F). No significant difference was observed in m^{6}A levels at these off-target sites between cells expressing the dCasRx–m^{6}A editors and the control cells (Fig. 3G-J). Three of the sequences (*RUNX family transcription factor 2*, *potassium voltage-gated channel subfamily D member 2* [*KCND2*], and *spermatogenesis and oogenesis-specific basic helix-loop-helix 2*) exhibited a slight increase in methylation levels in cells expressing dCasRx–METTL3-CD and ITGA6-multi-gRNA, while two (*KCND2* and myotubularin-related protein 1) demonstrated slightly decreased methylation in cells expressing dCasRx–ALKBH5-CD and ITGA6-multi-gRNA (Fig. 3G-J), indicating limited off-target effects. To determine whether the dCasRx–m^{6}A editors altered the distribution of transcriptome-wide RNA methylation, we performed meRIP-seq using cell lines stably expressing both the dCasRx–m^{6}A editors and ITGA6-multi-gRNA. Compared with the control groups expressing "λ2" gRNA, those with dCasRx–METTL3-CD and ITGA6-multi-gRNA exhibited only slight increase in the m^{6}A levels of 1090 additional genes out of the 20,612 tested (5.3 %; Supplementary Fig. S5A and B), whereas those with dCasRx–ALKBH5-CD and ITGA6-multi-gRNA exhibited a mar-

ginal reduction in the m^{6}A levels of 1084 additional genes out of a total 16,869 (6.4 %; Supplementary Fig. S5C and D).These findings indicate that the dCasRx–m^{6}A editors have a satisfactory on-target efficiency.

Multi-target demethylation using dCasRx–ALKBH5-CD with ITGA6-multi-gRNA reduces ITGA6 translation

We previously suggested the presence of four m^{6}A-modification sites (#96, #111, #195, and #233) in the 3′ UTR of *ITGA6* mRNA and that m^{6}A promotes ITGA6 translation(18). To investigate whether dCasRx–ALKBH5-CD with ITGA6-multi-gRNA targeting of the four m^{6}A sites reduces *ITGA6* translation, we performed western blot and RT-qPCR assays using stable cell lines. Western blot results revealed that dCasRx–ALKBH5-CD, not dCasRx-dALKBH5-CD, with ITGA6-multi-gRNA suppressed ITGA6 levels relative to those observed in the control group (Fig. 4A and B), whereas *ITGA6* mRNA levels did not differ between the groups (Fig. 4C). In addition, to assess the expression of ITGA6 in cells transfected with dCasRx–METTL3-CD or dCasRx -ALKBH5-CD, western blot experiments were conducted. The results showed that the expression of ITGA6 was unchanged when dCasRx–METTL3-CD or dCasRx -ALKBH5-CD was overexpressed alone (Supplementary Fig. S6), suggesting that gRNA was required for the biological effects of dCasRx–METTL3-CD and dCasRx -ALKBH5-CD. Polyribosome–RT-qPCR analysis of *ITGA6* mRNA abundance in the polysome confirmed that dCasRx–ALKBH5-CD suppressed the translational efficiency of *ITGA6*, with similar efficiency observed in monosomes (Fig. 4D and Supplementary Fig. S7). These data indicate that dCasRx–ALKBH5-CD downregulate *ITAG6* expression at the translational level.

Multi-target demethylation of ITGA6 mRNA inhibits BCa progression

We previously reported that m^{6}A modification of *ITGA6* mRNA promotes BCa development and progression(18). To assess whether multi-target demethylation of *ITGA6* mRNA by dCasRx–ALKBH5-CD can reverse or inhibit BCa progression, we first performed migration, proliferation, and sphere-formation assays using lentivirus-infected cell lines stably expressing dCasRx–ALKBH5-CD and ITGA6-multi-gRNA. The results confirmed that multi-target demethylation of *ITGA6* mRNA using dCasRx–ALKBH5-CD with ITGA6-multi-gRNA, but not dCasRx-dALKBH5-CD, significantly suppressed the migration, proliferation, and sphere-formation properties of T24 cells (Fig. 5A–E; Supplementary Fig. S8 and S9). Next, transwell assay was conducted to assess capacity of invasion. The result showed that dCasRx–ALKBH5-CD with ITGA6-multi-gRNA down-regulated the invasion of T24 cells (Supplementary Fig. S10). We then performed subcutaneous tumor-formation experiments in nude mice to determine the influence of dCasRx–ALKBH5-CD on BCa progression. Cells stably expressing dCasRx–ALKBH5-CD and ITGA6-multi-gRNA possessed markedly worse tumorigenic capacity relative to the control cells (Fig. 5F–H), whereas dCasRx-dALKBH5-CD did not affect cell tumorigenicity (Fig. 5F–H). Additionally, we used a tail-vein metastatic assay to assess the *in vivo* effect of multi-target *ITGA6* demethylation on T24 cell metastasis. Fewer lung metastatic nodules were observed in mice in the ITGA6-multi-gRNA group relative to those in the control mice in the λ2 gRNA group (Fig. 5I and J). These results show that multi-target demethylation of *ITGA6* significantly reduces the metastatic ability of T24 cells. Collectively, these *in vitro* and *in vivo* results demonstrate the ability of multi-target demethylation of *ITGA6* mRNA by dCasRx–ALKBH5-CD to inhibit BCa progression.

AAV2/8 delivery of dCasRx–ALKBH5-CD and ITGA6-multi-gRNA inhibits BCa progression

The dCasRx–ALKBH5-CD fusion protein comprises 1227 amino acids, which allow its packaging into an AAV2/8 vector. We designed an AAV vector (AAV$^{\text{ITGA6-multi-gRNA}}$) capable of simultaneously targeting four m^{6}A sites on *ITGA6* mRNA (Fig. 1B). To evaluate

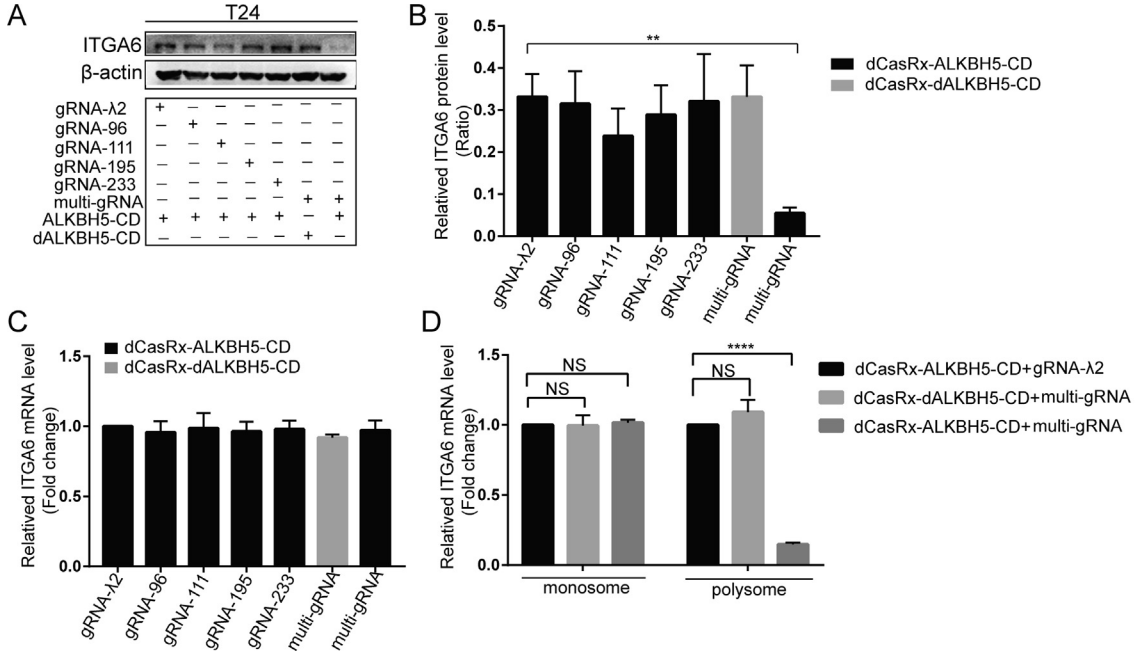

Fig. 4. Multi-target demethylation using dCasRx-ALKBH5-CD reduces translation. (A) Western blot analysis of ITGA6 expression in the controls (T24 cells with dCasRx-ALKBH5-CD and λ2-gRNA; T24 cells with dCasRx-dALKBH5-CD and ITGA6-multi-gRNA) and T24 cells transfected with dCasRx-ALKBH5-CD and ITGA6-gRNAs. (B) Statistical analysis of relative protein expression of *ITGA6*. (C) qPCR analysis of *ITGA6* mRNA expression. (D) Polyribosome analysis of *ITGA6* RNA expression in cells transfected with dCasRx-ALKBH5-CD, dCasRx-dALKBH5-CD, λ2-gRNA, or ITGA6-multi-gRNA. $^{**}P < 0.0001$, $^{****}P < 0.0001$.

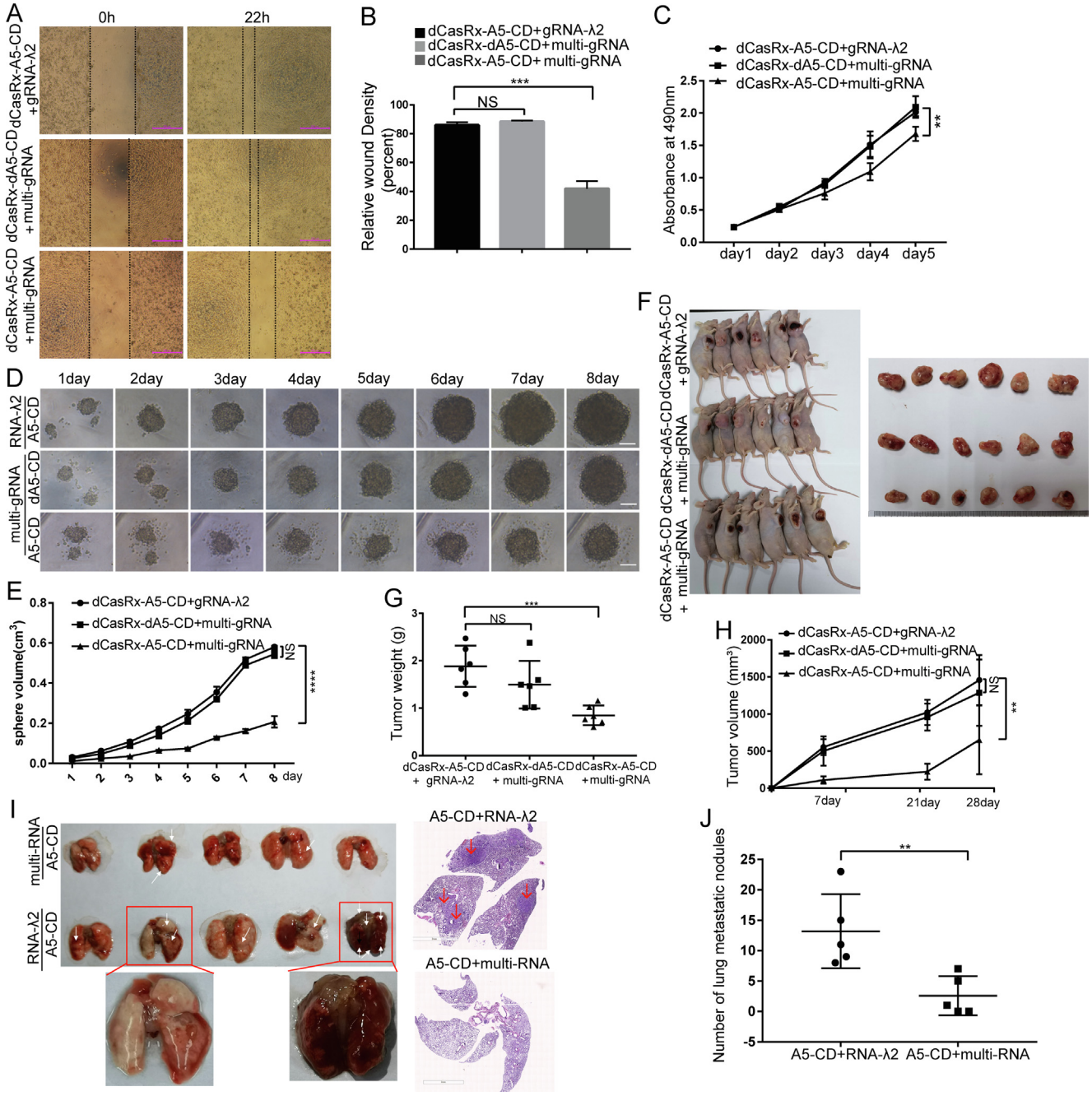

Fig. 5. Multi-target demethylation at *ITGA6* mRNA inhibits bladder cancer progression. (A–E). Migration (A, B), proliferation(C) and sphere formation (D) properties of T24 cells with multi-target demethylation at ITGA6 using dCasRx-ALKBH5-CD and ITGA6-multi-gRNA. (E) statistical analysis of sphere formation. (F–H) Subcutaneous tumor formation assay in nude mice injected with dCasRx-ALKBH5-CD and ITGA6-multi-gRNA. Representative tumor images (F), tumor weight (G), and tumor growth curves (H) (n = 6 per group). (I, J) Tail vein injection of dCasRx-ALKBH5-CD and ITGA6-multi-gRNA. Representative pulmonary nodule images (I) and statistical analysis of pulmonary nodules (J) (n = 5 per group). The experiments repeated three times. $^{**}P < 0.01$, $^{***}P < 0.001$. (A: Scale bar, 500 μm; D: Scale bar, 10 μm; I: Scale bar, 3 mm).

the efficacy of the AAV vectors, we subcutaneously implanted T24 cells into nude mice, and 1-week later, intratumorally injected AAV2/8$^{dCasRx\text{-}ALKBH5\text{-}CD}$ and AAV2/8$^{ITGA6\text{-}multi\text{-}gRNA}$ thrice every 2 days (Fig. 6A), with AAV2/8^{GFP} used as a negative control. Compared with that in the AAV2/8^{GFP}-treated mice, administration of AAV2/8$^{dCasRx\text{-}ALKBH5\text{-}CD}$ combined with AAV2/8$^{ITGA6\text{-}multi\text{-}gRNA}$ inhibited tumor growth in experimental mice (Fig. 6B and C). As expected, AAV2/8$^{dCasRx\text{-}ALKBH5\text{-}CD}$ along with AAV2/8$^{ITGA6\text{-}multi\text{-}gRNA}$ administration efficiently and specifically downregulated *ITGA6* (Fig. 6D). Notably, delivery of both the vectors did not induce liver or kidney damage (Fig. 6E and F), suggesting that AAV2/8 did not elicit biological toxicity. These results indicate that AAV delivery of dCasRx–ALKBH5-CD and ITGA6-multi-gRNA effectively and safely suppresses BCa tumor growth.

Discussion

Studies on the regulatory mechanism of m^{6}A have reported aberrant m^{6}A modification as a novel potential pathogenic mechanism for various diseases, including cancer [18,19,34,35] In BCa, m^{6}A modifications regulate various genes necessary for tumorigenesis [36–41]. Therefore, targeting the dysregulated m^{6}A regula-

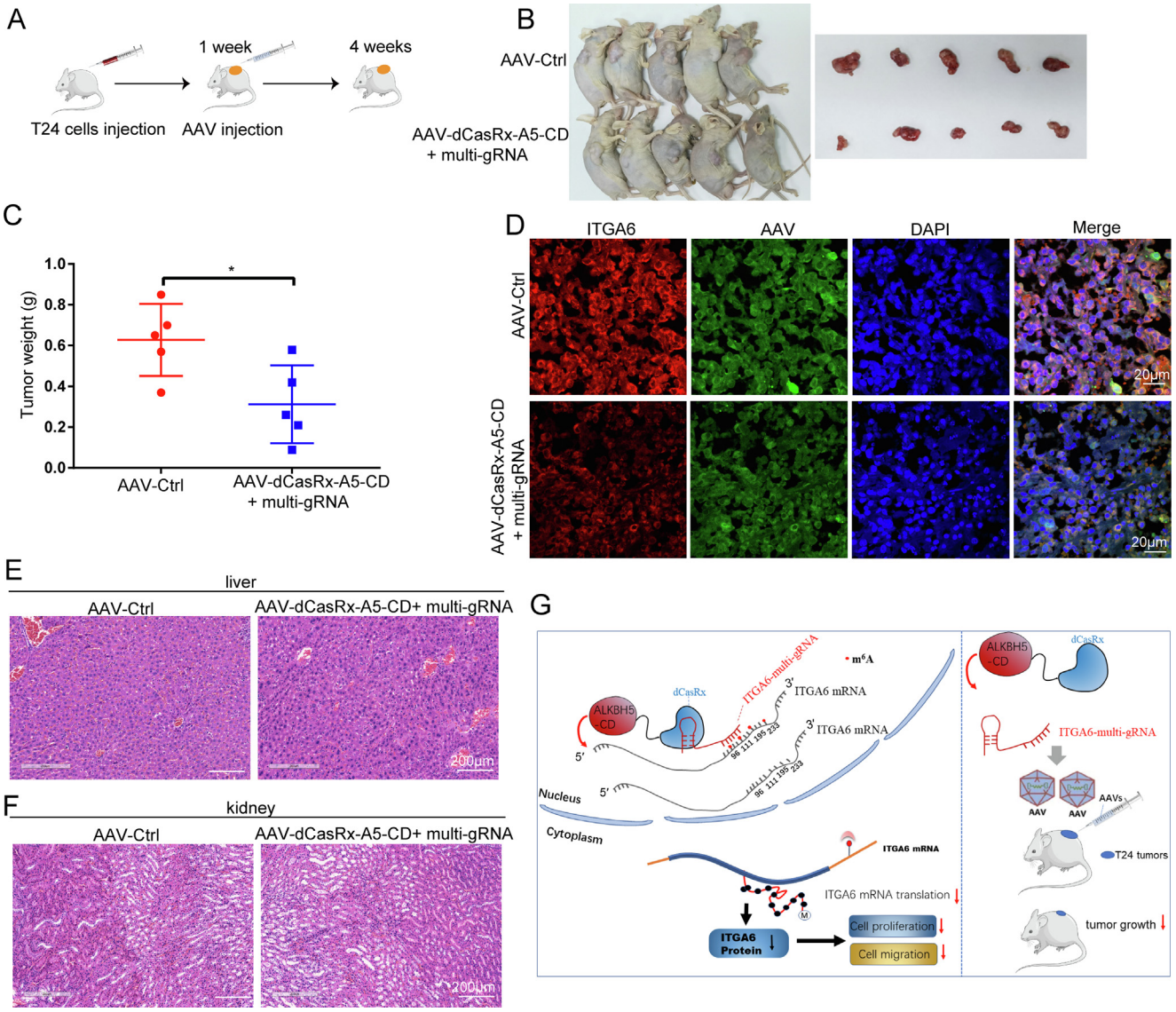

Fig. 6. AAV2/8-delivery of dCasRx-ALKBH5-CD and ITGA6-multi-gRNA inhibits the progression of bladder cancer. (A). Schematic representation of AAV2/8-mediated delivery of dCasRx-ALKBH5-CD and ITGA6-multi-gRNA to mice. (B) Representative tumor images of T24 tumor-loaded mice treated with AAV (n = 6). (C) Statistical analysis of tumor weights for T24 tumor-loaded mice treated with AAV. (D) Immunofluorescence analysis of ITGA6 levels in mice treated with AAV. (E, F) Hematoxylin and eosin staining of the kidney and liver tissues from T24 tumor-loaded mice treated with AAV. (G)The schematic model of the effects and underlying mechanism of the multisite dCasRx–m^{6}A editor targeted m^{6}A demethylation of ITGA6 mRNA in BC growth and progression. *P < 0.05. (D: Scale bars, 20 μm; E, F: Scale bars, 200 μm).

tors represents a promising strategy for cancer therapy. In the present study, we developed the multisite dCasRx–m^{6}A editor and demonstrated that subsequent multi-target demethylation of *ITGA6* mRNA inhibits BCa progression, indicating that the multisite dCasRx–m^{6}A editor represents a novel tool with potential efficacy in cancer therapy.

Recently, several studies have reported the targeting of m^{6}A modifications based on CRISPR technology. For instance, Liu et al. [42] reported that m^{6}A 'writers' or m^{6}A 'erasers' fused to CRISPR-Cas9 can achieve site-specific methylation or demethylation in the presence of gRNA. We previously generated a construct in which METTL3 CD (METTL3-CD) was fused to the *N*-terminus of dCas9 to mediate efficient site-specific m^{6}A installation to investigate the site-specific effects of mRNA methylation with a cognate sgRNA and PAM-mer [43]. Meanwhile, Zhen et al. [28] developed dCasRx epitranscriptomic editors that enable site-specific m^{6}A installation or removal at a single locus. Furthermore, Wilson et al. [27] fused nucleus-localized dCas13 with a truncated METTL3 methyltransferase domain and found that the fusion protein induced site-specific m^{6}A incorporation at a single site with low off-target effects. A fusion protein, generated by linking inactive Cas13b to ALKBH5, also exhibited efficient demethylation of targeted genes with a low off-target activity [44]. Indeed, several lines of evidence have revealed multiple m^{6}A sites on a transcript that cooperatively regulate mRNA fate. For example, m^{6}A modification of multiple genes, or multiple m^{6}A modifications of the same gene, can affect cancer occurrence and development [18,19,45]. It is, therefore, essential to develop a novel strategy for investigating the multisite synergistic effects of m^{6}A in cancer.

In this study, we combined the RNA-targeting capability of CRISPR-Cas13Rx with the RNA methyltransferase METTL3 CD (METTL3-CD) or demethylase ALKBH5 CD (ALKBH5-CD) to create a targeted methylation system that can be programmed to modify the epitranscriptome. We previously identified four m^{6}A-modification sites in the 3′ UTR of *ITGA6* mRNA and reported that m^{6}A modification of the four sites cooperatively regulates *ITAG6*

translation. However, it is challenging to deliver multiple gRNAs efficiently and simultaneously for m^{6}A manipulation. Therefore, it is important to develop a single gRNA vector capable of simultaneously targeting multiple sites. To address this issue, we developed a lentiviral-multi-gRNA or AAV-multi-gRNA vector with four independent Pol III promoters; each promoter drives the expression of one *ITGA6* CasRx gRNA. Each gRNA is efficiently expressed at a similar level. To determine whether the dCasRx–m^{6}A editors altered the distribution of transcriptome-wide RNA methylation, we performed meRIP-seq and found that dCasRx–METTL3-CD and ITGA6-multi-gRNA exhibited only slight increase in the m^{6}A levels (5.3 %; Supplementary Fig. S5A and B), whereas dCasRx–ALKBH5-CD and ITGA6-multi-gRNA exhibited a marginal reduction in the m^{6}A levels (6.4 %; Supplementary Fig. S5C and D). Zhen Xia [28] et al also conducted transcriptome-wide RNA methylation alters by meRIP-seq. their results showed that compared to the control group, dCasRx-METTL3 with target sgRNA mildly increased m^{6}A level (10.4 %), while dCasRx-ALKBH5 only decreases m^{6}A levels (1.6 %), suggesting a low off-target effects of the dCasRx epitranscriptomic platform. We used the same screening conditions (FDR-corrected $p < 0.05$ and > 4-fold change). Our dCasRx–m^{6}A editors with ITGA6-multi-gRNA enabled site-specific m^{6}A insertion or removal at the four target sites with low off-target effects.

Remarkably, the small sizes of the dCasRx–METTL3-CD and dCasRx–ALKBH5-CD allow them to be packaged into lentiviral vectors and even into AAV vectors for gene therapy. Here, we used lentiviral vectors to investigate the *in vitro* and *in vivo* functions of dCasRx–ALKBH5-CD with ITGA6-multi-gRNA in BCa, revealing that combined application of dCasRx–ALKBH5-CD and lentiviral-multi-gRNA effectively and simultaneously targeted four m^{6}A sites in *ITGA6* mRNA, thereby inhibiting BCa cell proliferation and migration. Importantly, we also used AAV to deliver dCasRx–ALKBH5-CD and ITGA6-multi-gRNA into nude mice bearing T24 tumors for therapeutic intervention. Our results demonstrated that AAV2/8$^{dCasRx\text{-}ALKBH5CD}$/AAV2/8$^{ITGA6\text{-}multi\text{-}gRNA}$ suppressed tumor growth, indicating that our multisite dCasRx m^{6}A-modification systems have potential efficacy in cancer therapy.

In summary, this study demonstrates for the first time that multisite dCasRx–m^{6}A editors can achieve multisite, targeted modification of mRNA. Specifically, we show that delivery of dCasRx–ALKBH5-CD along with ITGA6-multi-gRNA inhibits BCa cell proliferation and tumor development. Importantly, the results showing that *in vivo* administration of AAV2/8$^{dCasRx\text{-}ALKBH5CD}$ and AAV2/8$^{-ITGA6\text{-}multi\text{-}gRNA}$ reduces BCa progression.

Conclusion

Our study suggests this technology to be a novel tool for exploring the biological effects of multisite-specific m^{6}A RNA methylation, as well as a promising strategy for clinical applications targeting BCa or RNA-associated diseases.

Data sharing statement

MeRIP-seq data generated in this study have been deposited to the NCBI Sequence Read Archive (SRA) under accession number PRJNA853447.

Compliance with Ethics Requirements

All Institutional and National Guidelines for the care and use of animals (fisheries) were followed.

Declaration of Competing Interest

The authors declare that they have no known competing financial interests or personal relationships that could have appeared to influence the work reported in this paper.

Acknowledgments

This work was supported by the National Natural Science Foundation of China (82073047, 82272995 and 81772699), Guangdong Provincial Joint Fund Youth Project (2020A1515110117), and China Postdoctoral Science Foundation (2020M683074).

Appendix A. Supplementary material

Supplementary data to this article can be found online at https://doi.org/10.1016/j.jare.2023.03.010.

References

[1] Bray F, Ferlay J, Soerjomataram I, Siegel RL, Torre LA, Jemal A. Global cancer statistics 2018: GLOBOCAN estimates of incidence and mortality worldwide for 36 cancers in 185 countries. CA Cancer J Clin 2018;68:394–424. doi: https://doi.org/10.3322/caac.21492.

[2] Compérat E, Larré S, Roupret M, Neuzillet Y, Pignot G, Quintens H, et al. Clinicopathological characteristics of urothelial bladder cancer in patients less than 40 years old. Virchows Arch 2015;466:589–94. doi: https://doi.org/10.1007/s00428-015-1739-2.

[3] Charlton ME, Adamo MP, Sun L, Deorah S. Bladder cancer collaborative stage variables and their data quality, usage, and clinical implications: a review of SEER data, 2004–2010. Cancer 2014;120(Suppl 23):3815–25. doi: https://doi.org/10.1002/cncr.29047.

[4] Sylvester RJ, van der Meijden AP, Oosterlinck W, Witjes JA, Bouffioux C, Denis L et al. Predicting recurrence and progression in individual patients with stage Ta T1 bladder cancer using EORTC risk tables: a combined analysis of 2596 patients from seven EORTC trials. Eur Urol. 2006; 49: 466-465; discussion 475-467. https://doi.org/10.1016/j.eururo.2005.12.031.

[5] Seidl C. Targets for Therapy of Bladder Cancer. Semin Nucl Med 2020;50:162–70. doi: https://doi.org/10.1053/j.semnuclmed.2020.02.006.

[6] Lei T, Zhao X, Jin S, Meng Q, Zhou H, Zhang M. Discovery of potential bladder cancer biomarkers by comparative urine proteomics and analysis. Clin Genitourin Cancer 2013;11:56–62. doi: https://doi.org/10.1016/j.clgc.2012.06.003.

[7] Niu Y, Wan A, Lin Z, Lu X, Wan G. N (6)-Methyladenosine modification: a novel pharmacological target for anti-cancer drug development. Acta Pharm Sin B 2018;8:833–43. doi: https://doi.org/10.1016/j.apsb.2018.06.001.

[8] Chen XY, Zhang J, Zhu JS. The role of m(6)A RNA methylation in human cancer. Mol Cancer 2019;18:103. doi: https://doi.org/10.1186/s12943-019-1033-z.

[9] Gilbert WV, Bell TA, Schaening C. Messenger RNA modifications: Form, distribution, and function. Science 2016;352:1408–12. doi: https://doi.org/10.1126/science.aad8711.

[10] Lipshitz HD, Claycomb JM, Smibert CA. Post-transcriptional regulation of gene expression. Methods 2017;126:1–2. doi: https://doi.org/10.1016/j.ymeth.2017.08.007.

[11] Roignant JY, Soller M. m(6)A in mRNA: An Ancient Mechanism for Fine-Tuning Gene Expression. Trends Genet 2017;33:380–90. doi: https://doi.org/10.1016/j.tig.2017.04.003.

[12] Shi H, Wang X, Lu Z, Zhao BS, Ma H, Hsu PJ, et al. YTHDF3 facilitates translation and decay of N(6)-methyladenosine-modified RNA. Cell Res 2017;27:315–28. doi: https://doi.org/10.1038/cr.2017.15.

[13] Niu Y, Zhao X, Wu YS, Li MM, Wang XJ, Yang YG. N6-methyl-adenosine (m6A) in RNA: an old modification with a novel epigenetic function. Genom Proteomics Bioinform 2013;11:8–17. doi: https://doi.org/10.1016/j.gpb.2012.12.002.

[14] Li T, Hu PS, Zuo Z, Lin JF, Li X, Wu QN, et al. METTL3 facilitates tumor progression via an m(6)A-IGF2BP2-dependent mechanism in colorectal carcinoma. Mol Cancer 2019;18:112. doi: https://doi.org/10.1186/s12943-019-1038-7.

[15] Wang Q, Chen C, Ding Q, Zhao Y, Wang Z, Chen J, et al. METTL3-mediated m(6)A modification of HDGF mRNA promotes gastric cancer progression and has prognostic significance. Gut 2020;69:1193–205. doi: https://doi.org/10.1136/gutjnl-2019-319639.

[16] Yue B, Song C, Yang L, Cui R, Cheng X, Zhang Z, et al. METTL3-mediated N6-methyladenosine modification is critical for epithelial-mesenchymal transition and metastasis of gastric cancer. Mol Cancer 2019;18:142. doi: https://doi.org/10.1186/s12943-019-1065-4.

[17] Cheng M, Sheng L, Gao Q, Xiong Q, Zhang H, Wu M, et al. The m(6)A methyltransferase METTL3 promotes bladder cancer progression via AFF4/NF-κB/MYC signaling network. Oncogene 2019;38:3667–80. doi: https://doi.org/10.1038/s41388-019-0683-z.

[18] Jin H, Ying X, Que B, Wang X, Chao Y, Zhang H, et al. N(6)-methyladenosine modification of ITGA6 mRNA promotes the development and progression of bladder cancer. EBioMedicine 2019;47:195–207. doi: https://doi.org/10.1016/j.ebiom.2019.07.068.
[19] Yang F, Jin H, Que B, Chao Y, Zhang H, Ying X, et al. Dynamic m(6)A mRNA methylation reveals the role of METTL3-m(6)A-CDCP1 signaling axis in chemical carcinogenesis. Oncogene 2019;38:4755–72. doi: https://doi.org/10.1038/s41388-019-0755-0.
[20] Yu H, Yang X, Tang J, Si S, Zhou Z, Lu J, et al. ALKBH5 Inhibited Cell Proliferation and Sensitized Bladder Cancer Cells to Cisplatin by m6A-CK2α-Mediated Glycolysis. Mol Ther Nucleic Acids 2021;23:27–41. doi: https://doi.org/10.1016/j.omtn.2020.10.031.
[21] Brooks DL, Schwab LP, Krutilina R, Parke DN, Sethuraman A, Hoogewijs D, et al. ITGA6 is directly regulated by hypoxia-inducible factors and enriches for cancer stem cell activity and invasion in metastatic breast cancer models. Mol Cancer 2016;15:26. doi: https://doi.org/10.1186/s12943-016-0510-x.
[22] Stewart RL, West D, Wang C, Weiss HL, Gal T, Durbin EB, et al. Elevated integrin α6β4 expression is associated with venous invasion and decreased overall survival in non-small cell lung cancer. Hum Pathol 2016;54:174–83. doi: https://doi.org/10.1016/j.humpath.2016.04.003.
[23] Ammothumkandy A, Maliekal TT, Bose MV, Rajkumar T, Shirley S, Thejaswini B, et al. CD66 and CD49f expressing cells are associated with distinct neoplastic phenotypes and progression in human cervical cancer. Eur J Cancer 2016;60:166–78. doi: https://doi.org/10.1016/j.ejca.2016.03.072.
[24] Abudayyeh OO, Gootenberg JS, Essletzbichler P, Han S, Joung J, Belanto JJ, et al. RNA targeting with CRISPR-Cas13. Nature 2017;550:280–4. doi: https://doi.org/10.1038/nature24049.
[25] Konermann S, Lotfy P, Brideau NJ, Oki J, Shokhirev MN, Hsu PD. Transcriptome Engineering with RNA-Targeting Type VI-D CRISPR Effectors. Cell 2018;173:665–676.e614. doi: https://doi.org/10.1016/j.cell.2018.02.033.
[26] Zhou H, Su J, Hu X, Zhou C, Li H, Chen Z, et al. Glia-to-Neuron Conversion by CRISPR-CasRx Alleviates Symptoms of Neurological Disease in Mice. Cell 2020;181:590–603.e516. doi: https://doi.org/10.1016/j.cell.2020.03.024.
[27] Wilson C, Chen PJ, Miao Z, Liu DR. Programmable m(6)A modification of cellular RNAs with a Cas13-directed methyltransferase. Nat Biotechnol 2020;38:1431–40. doi: https://doi.org/10.1038/s41587-020-0572-6.
[28] Xia Z, Tang M, Ma J, Zhang H, Gimple RC, Prager BC, et al. Epitranscriptomic editing of the RNA N6-methyladenosine modification by dCasRx conjugated methyltransferase and demethylase. Nucleic Acids Res 2021;49:7361–74. doi: https://doi.org/10.1093/nar/gkab517.
[29] Liu W, Yan J, Zhang Z, Pian H, Liu C, Li Z. Identification of a selective DNA ligase for accurate recognition and ultrasensitive quantification of N(6)-methyladenosine in RNA at one-nucleotide resolution. Chem Sci 2018;9:3354–9. doi: https://doi.org/10.1039/c7sc05233b.
[30] Xiao Y, Wang Y, Tang Q, Wei L, Zhang X, Jia G. An Elongation- and Ligation-Based qPCR Amplification Method for the Radiolabeling-Free Detection of Locus-Specific N(6) -Methyladenosine Modification. Angew Chem Int Ed Engl 2018;57:15995–6000. doi: https://doi.org/10.1002/anie.201807942.
[31] Zhang Z, Chen LQ, Zhao YL, Yang CG, Roundtree IA, Zhang Z, et al. Single-base mapping of m(6)A by an antibody-independent method. Sci Adv 2019;5:eaax0250. doi: https://doi.org/10.1126/sciadv.aax0250.
[32] Ying X, Liu B, Yuan Z, Huang Y, Chen C, Jiang X, et al. METTL1-m(7) G-EGFR/EFEMP1 axis promotes the bladder cancer development. Clin Transl Med 2021;11:e675.
[33] Kabadi AM, Ousterout DG, Hilton IB, Gersbach CA. Multiplex CRISPR/Cas9-based genome engineering from a single lentiviral vector. Nucleic Acids Res 2014;42:e147.
[34] Deng X, Su R, Feng X, Wei M, Chen J. Role of N(6)-methyladenosine modification in cancer. Curr Opin Genet Dev 2018;48:1–7. doi: https://doi.org/10.1016/j.gde.2017.10.005.
[35] Lin S, Choe J, Du P, Triboulet R, Gregory RI. The m(6)A Methyltransferase METTL3 Promotes Translation in Human Cancer Cells. Mol Cell 2016;62:335–45. doi: https://doi.org/10.1016/j.molcel.2016.03.021.
[36] Chen M, Nie ZY, Wen XH, Gao YH, Cao H, Zhang SF. m6A RNA methylation regulators can contribute to malignant progression and impact the prognosis of bladder cancer. Biosci Rep 2019:39. doi: https://doi.org/10.1042/bsr20192892.
[37] Han J, Wang JZ, Yang X, Yu H, Zhou R, Lu HC, et al. METTL3 promote tumor proliferation of bladder cancer by accelerating pri-miR221/222 maturation in m6A-dependent manner. Mol Cancer 2019;18:110. doi: https://doi.org/10.1186/s12943-019-1036-9.
[38] Tao L, Mu X, Chen H, Jin D, Zhang R, Zhao Y, et al. FTO modifies the m6A level of MALAT and promotes bladder cancer progression. Clin Transl Med 2021;11:e310.
[39] Wei W, Sun J, Zhang H, Xiao X, Huang C, Wang L, et al. Circ0008399 Interaction with WTAP Promotes Assembly and Activity of the m(6)A Methyltransferase Complex and Promotes Cisplatin Resistance in Bladder Cancer. Cancer Res 2021;81:6142–56. doi: https://doi.org/10.1158/0008-5472.Can-21-1518.
[40] Xie H, Li J, Ying Y, Yan H, Jin K, Ma X, et al. METTL3/YTHDF2 m(6) A axis promotes tumorigenesis by degrading SETD7 and KLF4 mRNAs in bladder cancer. J Cell Mol Med 2020;24:4092–104. doi: https://doi.org/10.1111/jcmm.15063.
[41] Yan R, Dai W, Wu R, Huang H, Shu M. Therapeutic targeting m6A-guided miR-146a-5p signaling contributes to the melittin-induced selective suppression of bladder cancer. Cancer Lett 2022;534:. doi: https://doi.org/10.1016/j.canlet.2022.215615215615.
[42] Liu XM, Zhou J, Mao Y, Ji Q, Qian SB. Programmable RNA N(6)-methyladenosine editing by CRISPR-Cas9 conjugates. Nat Chem Biol 2019;15:865–71. doi: https://doi.org/10.1038/s41589-019-0327-1.
[43] Ying X, Jiang X, Zhang H, Liu B, Huang Y, Zhu X, et al. Programmable N6-methyladenosine modification of CDCP1 mRNA by RCas9-methyltransferase like 3 conjugates promotes bladder cancer development. Mol Cancer 2020;19:169. doi: https://doi.org/10.1186/s12943-020-01289-0.
[44] Li J, Chen Z, Chen F, Xie G, Ling Y, Peng Y, et al. Targeted mRNA demethylation using an engineered dCas13b-ALKBH5 fusion protein. Nucleic Acids Res 2020;48:5684–94. doi: https://doi.org/10.1093/nar/gkaa269.
[45] Deng X, Su R, Weng H, Huang H, Li Z, Chen J. RNA N(6)-methyladenosine modification in cancers: current status and perspectives. Cell Res 2018;28:507–17. doi: https://doi.org/10.1038/s41422-018-0034-6.